RSC Sustainability

ROYAL SOCIETY OF CHEMISTRY

PAPER

View Article Online
View Journal | View Issue

Cite this: *RSC Sustainability*, 2023, **1**, 543

Bio-based vitrimers from divanillic acid and epoxidized soybean oil†

Yunfan Zhang, Enomoto Yukiko and Iwata Tadahisa *

Received 21st December 2022
Accepted 5th March 2023

DOI: 10.1039/d2su00140c

rsc.li/rscsus

Divanillic acid (DVA), a symmetrical dimer of vanillic acid, is a novel aromatic building block for bio-based polymers. In the present study, we prepared DVA-derived crosslinked vitrimers, which constitute a new class of thermosetting polymers formed *via* dynamic covalent bonds. We cured two series of bio-based vitrimers, OHESO-*x* and BuESO-*x* (*x* represents the COOH/epoxy ratio, $x = 1.5$, 1.0, 0.7) derived from DVA and butoxylated DVA, respectively, with epoxidized soybean oil (ESO) in the presence of a transesterification catalyst. Depending on the side chain structures and *x* values, the glass transition temperatures (T_gs) and Young's moduli of the vitrimer films varied from 20 to 62 °C and from 3 to 286 MPa, respectively. The OHESO-*x* vitrimers had higher T_gs and Young's moduli than the BuESO-*x* vitrimers with the same *x* values. This was due to the hydrogen bonds formed by the free phenolic hydroxyl groups and unreacted carboxylic acid groups. We confirmed dynamic transesterification by stress relaxation testing, and characterized the reprocessability and self-healing properties of the vitrimers.

Sustainability spotlight

Bio-based polymers have received considerable attention in both academia and industry owing to their outstanding environmental benignity. However, most commercialized bio-based polymers are aliphatic polyesters, such as poly(lactic acid) and poly(butylene succinate), which fail to satisfy all market demands because of their limited thermal and mechanical properties. As a result, there has been growing interest in using bio-based aromatics to develop bio-based aromatic polymers with enhanced material properties. This work focused on developing high-performance and recyclable polymeric materials using renewable natural feedstocks by applying the concept of vitrimer, which is a class of polymers crosslinked *via* dynamic covalent bonds. It aligns with the UN's Sustainable Development Goals 12 (responsible consumption and production), 13 (climate action) and 15 (life on land).

1 Introduction

The world is currently facing some tough challenges, such as global energy supply and environmental issues. Therefore, polymeric materials made from renewable natural feedstocks (*i.e.*, bio-based polymers) are attracting burgeoning attention worldwide owing to their huge potential as alternatives to petroleum-based polymers.[1,2] Representative bio-based polymers include aliphatic bio-based polyesters derived from the fermentation products of carbohydrates, such as poly(lactic acid) (PLA) and poly(butylene succinate) (PBS), which have been extensively studied and industrialized.[3,4] Recently, researchers have focused on biomass-derived aromatics with the aim of obtaining high-performance aromatic polymers with versatile applicability. For example, poly(ethylene furandicarboxylate) has received considerable interest owing to its outstanding thermal and gas barrier properties.[5,6] The use of lignin fragments or other plant-derived aromatics, such as vanillic acid[7,8] and gallic acid,[9] to prepare polymers is also a current trend.

We recently systematically synthesized and characterized aromatic bio-based polymers derived from divanillic acid (DVA), which is a symmetrical dimer of vanillic acid, such as polyesters,[10–13] polyamides,[14,15] and polyketones.[16] DVA and divanillin (DV) are seen as promising bio-based building blocks because they can be synthesized using enzymes as green catalysts,[17,18] and their biphenyl structures increase the rigidity of the polymer chains, thereby endowing the material with favorable thermal and mechanical properties. Nevertheless, according to previous works by Cramail *et al.*[19–22] and our own group, it is challenging to use DVA or DV to prepare polymers directly. The free phenolic hydroxyl groups are usually alkoxylated to enhance the miscibility of DVA/DV with other comonomers. Therefore, the preparation of DVA/DV-derived polymers is not sufficiently cost-effective. Furthermore, unlike some conventional aromatic polymers such as poly(ethylene terephthalate), linear DVA/DV-derived polymers, especially DVA-derived polyesters, are virtually impossible to crystallize. This significantly limits their practical use. Cramail *et al.* proposed a new approach to preparing DV-derived polymers: the formation of

Department of Biomaterial Sciences, Graduate School of Agricultural and Life Sciences, The University of Tokyo, 1-1-1 Yayoi, Bunkyo-ku, Tokyo 113-8657, Japan. E-mail: atiwata@g.ecc.u-tokyo.ac.jp; Fax: +81-3-5841-1304; Tel: +81-3-58415266

† Electronic supplementary information (ESI) available: Product analysis, experimental details and supplementary figures. See DOI: https://doi.org/10.1039/d2su00140c

a thermosetting resin with a network topology cured from easy-to-prepare DV-based epoxy monomers.[23] Likewise, based on the material design strategies used for polyesters and epoxy resins,[24,25] we considered using DVA to prepare recyclable crosslinked polymers with favorable material performances by applying the concept of the vitrimer.

Vitrimers are a class of polymeric materials that are crosslinked by dynamic covalent bonds.[26,27] Under certain conditions (usually high temperature), bond exchange reactions occur and the molecular chains become mobile. The materials then become malleable and processable (*i.e.*, exhibit thermoplasticity). Because vitrimers undergo various types of bond exchange reactions, including transesterification,[26,28–31] transamination of vinylogous urethanes[32,33] and diketoenamines,[34] dioxaborolane metathesis,[35,36] silyl ether transalkoxylation[37] and metathesis[38] *etc.*, vitrimers provide more possibilities for the design and construction of polymer networks. Furthermore, vitrimers can be recycled by physical or chemical methods, and some of them are biodegradable.[35] Therefore, they are potential candidates for a new generation of eco-friendly crosslinked polymeric materials.

Bio-based vitrimers have received growing attention in recent years because they provide a facile means of utilizing biomass-derived compounds with multiple functional groups or complicated chemical structures.[39,40] For example, several research groups have prepared vitrimers from compounds or macromolecules such as rosin derivatives,[41,42] tannic acid,[43] and modified lignin;[44,45] they have little or no polymerizability (*i.e.*, are not suitable for traditional polymerization). Among the biomass-derived monomers, vanillin and epoxidized soybean oil (ESO) have been extensively studied as building blocks for bio-based vitrimers or other dynamically crosslinked polymers.[28,46–54] This is because vanillin has a relatively simple chemical structure among naturally occurring aromatics, and ESO is a low-cost, industrially produced epoxy. In many previous works, some petrochemicals or multiple reaction steps were still necessary to introduce exchangeable moieties (*e.g.*, vinylogous urethane and imine bonds) into the monomers. This fact made the process less environmentally friendly. In addition, although bio-based aliphatic acids, such as citric acid and sebacic acid, have been used to obtain transesterification-based vitrimers, there is a lack of research focusing on the direct use of bio-based aromatic acids as vitrimer monomers. Therefore, as we introduced earlier, DVA may offer a promising solution as a bio-based aromatic acid for the preparation of bio-based vitrimers with enhanced material properties.

In this present work, we prepared and characterized the fully bio-based vitrimers based on the dynamic transesterification of DVA or butoxylated DVA (BuDVA) and ESO. We cured DVA/BuDVA–ESO mixtures in the presence of zinc acetylacetonate hydrate (a transesterification catalyst), and subsequently fabricated vitrimer films. Next, we investigated the effects of the side chain (*i.e.*, the phenolic hydroxyl and butoxy groups of DVA and BuDVA, respectively) and the stoichiometric ratios of the carboxylic acid/epoxy groups on the thermal and mechanical properties of the vitrimers. At high temperatures, we confirmed transesterification by stress relaxation testing. We also determined the reprocessability, self-healing, and shape memory properties of the obtained vitrimers.

2 Experimental

2.1 Materials

Zinc acetylacetonate hydrate [$Zn(acac)_2$, 98%] and potassium hydroxide (KOH, >85%) were purchased from Wako Pure Chemical Industries, Ltd. The ESO (epoxide equivalent weight = 233.2 g eq.$^{-1}$) was generously donated by New Japan Chemical Co., Ltd. All other reagents were obtained commercially and used as received.

2.2 Synthesis of DVA and BuDVA

DVA and BuDVA were synthesized by the hydrolysis of dimethyl divanillate (Me-DVA) and dimethyl dibutoxy divanillate (Me-BuDVA) (Scheme 1); Me-DVA and Me-BuDVA were prepared according to the method we have used previously.[12]

DVA.[55] Me-DVA (10.00 g, 27.6 mmol, 1 equiv.) and KOH (12.38 g, 220.8 mmol, 8 equiv.) were dissolved in a tetrahydrofuran (THF)/water solution (350 mL, 1 : 1, v/v). After stirring the mixture at 70 °C overnight, the red aqueous layer was acidified with hydrochloric acid to induce precipitation. The precipitate was filtered, washed several times with deionized water, and dried *in vacuo* at. DVA was obtained as a pale orange solid (8.86 g, 96% yield).

BuDVA. Me-BuDVA (10.00 g, 21.1 mmol, 1 equiv.) and KOH (9.46 g, 168.6 mmol, 8 equiv.) were dissolved in 30 mL of methanol. After stirring the mixture at 40 °C overnight, we washed it with ethyl acetate, and acidified the colorless (or light yellow) aqueous layer with hydrochloric acid to induce precipitation. The precipitate was filtered, washed several times with deionized water, and dried *in vacuo* at 70 °C. BuDVA was obtained as a white powder (7.72 g, 82% yield).

2.3 Preparation of DVA/BuDVA–ESO vitrimers

As shown in Fig. 1, two series of vitrimers, named OHESO-*x* and BuESO-*x*, were prepared in the present study. OH and Bu represent the DVA (R = H) and BuDVA (R = Bu) monomers, respectively, and *x* represents the ratio of carboxylic acid (COOH) groups to epoxy groups (*i.e.*, *x* = COOH/epoxy, *n*/*n*). The formulation of the vitrimers is summarized in Table 1. We used 5 mol% (relative to the amount of COOH groups) of $Zn(acac)_2$ to catalyze the transesterification.

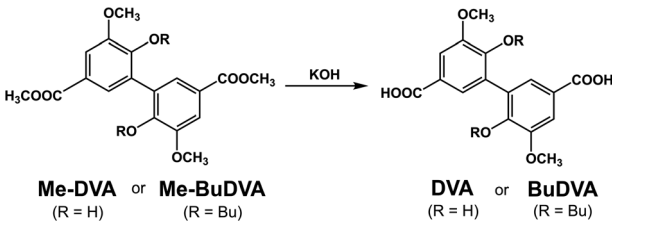

Scheme 1 Synthesis of divanillic acid (DVA) and dibutoxydivanillic acid (BuDVA).

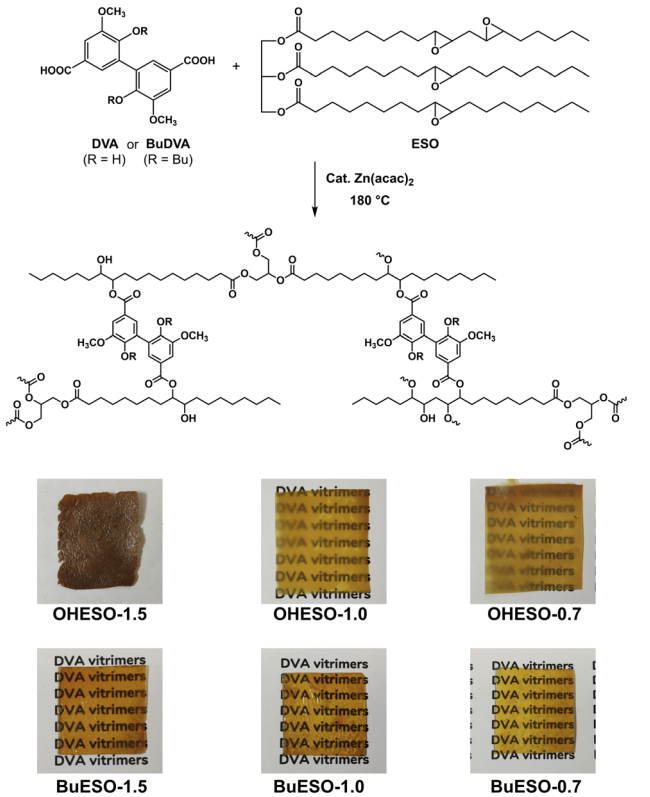

Fig. 1 Preparation and images of the DVA/BuDVA–ESO vitrimer films.

Table 1 Formulations of the DVA/BuDVA–ESO vitrimers

Codes	ESO (g)	Epoxy group (mmol)	Diacid	Diacid (g)	COOH group (mmol)	x^a
OHESO-0.7	2.00	8.57	DVA	1.00	6.00	0.7
OHESO-1.0				1.43	8.57	1.0
OHESO-1.5				2.15	12.86	1.5
BuESO-0.7	2.00	8.57	BuDVA	1.34	6.00	0.7
BuESO-1.0				1.91	8.57	1.0
BuESO-1.5				2.87	12.86	1.5

[a] $x = n$(COOH group)/n(epoxy group).

2.3.1 Preparation of OHESO-*x* vitrimer films. Predetermined amounts of DVA, ESO, $Zn(acac)_2$, and 10–20 mL of ethanol were introduced into a 50 mL round-bottom flask together. The resulting suspension was stirred vigorously at 60 °C for 10–20 min (it should be noted that the DVA only partially dissolved in the ethanol). The excess ethanol was then removed using a rotary evaporator, and the mixture was further dried in *vacuo* at 80 °C overnight. The mixtures when $x = 0.7$ and 1.0 comprised viscous brown slurries, and the mixture when $x = 1.5$ was a brown powder. Subsequently, the dried mixtures were sandwiched between two Teflon® sheets (0.2 mm thick) and cured at 180 °C for 6 h to form OHESO-*x* vitrimer films.

2.3.2 Preparation of BuESO-*x* vitrimer films. Predetermined amounts of BuDVA, ESO, $Zn(acac)_2$, and 10–20 mL of THF were introduced into a conical flask together and stirred at room temperature for 10–20 min. After the reactants had dissolved in the THF, the resulting solution was poured into a Teflon® Petri dish. When the THF had evaporated, the cast mixture was cured at 180 °C for 6 h without external pressure to form the BuESO-*x* vitrimer films.

2.4 Characterization

2.4.1 Nuclear magnetic resonance (NMR) spectroscopy. ^1H and ^{13}C NMR spectra of DVA and BuDVA were obtained using a JEOL JNM-A500 FT-NMR (500 MHz) spectrometer at 25 °C, with DMSO-d_6 as the solvent and tetramethylsilane as the internal standard.

2.4.2 Fourier-transform infrared (FT-IR) spectroscopy. FT-IR spectra of the monomers and vitrimers were obtained using an attenuated total reflectance Fourier-transform infrared (ATR FT-IR) spectrometer (FT/IR-6800; JASCO Co., Tokyo, Japan) in the range 400–4000 cm^{-1}. The powders or films of the samples were fixed on the diamond single-reflection ATR accessory (ATR Pro-one; JASCO Co., Tokyo, Japan) for measurement. We carried out 64 scans for each measurement.

2.4.3 Thermalgravimetric analysis (TGA). The thermal degradation temperatures of the vitrimers were determined using a TGA-50 instrument (Shimadzu, Japan). In each trial, a 3–6 mg film fragment was placed in an aluminum pan without a cover and heated from 30 to 550 °C at a rate of 20 °C min^{-1} under a nitrogen gas atmosphere.

2.4.4 Dynamical mechanical analysis (DMA). The glass transition temperatures (T_g) of the vitrimers were assessed using a DMA 8000 analyzer (PerkinElmer, USA) operating in single cantilever mode. In each trial, a slice of vitrimer film was loaded into a metal material pocket and heated from −30 to 220 °C under a nitrogen atmosphere. The heating rate and frequency were fixed at 3 °C min^{-1} and 1.0 Hz, respectively. The storage (E') and loss (E'') moduli, and the tan δ ($\tan\delta = E'/E''$) values were recorded.

2.4.5 Stress relaxation. The stress relaxation behaviors of the vitrimers were evaluated using an MCR 302 rheometer (Anton Paar, Austria) with a 25 mm parallel-plate (P25 kit) geometry. The measurements were conducted over a temperature range of 170–200 °C. The specimens were first heated to the corresponding temperatures and then held for 15 min to reach equilibrium. Subsequently, a strain of 3% was applied, and the relaxation modulus of each specimen was recorded as a function of time. An axial force of 15–20 N was applied to ensure a good contact between the specimen and the plate.

2.4.6 Tensile tests and film reprocessing. Tensile tests of vitrimer films were performed using an EZ-LX instrument (Shimadzu, Japan) at room temperature. The tensile speed was 10 mm min^{-1} and the initial gauge length was 10 mm. At least five tensile specimens (25 mm × 4 mm) were tested for each measurement. The maximum tensile strength (σ_{max}), maximum elongation (ε_{max}), and Young's modulus (E) were recorded. For OHESO-1.0 and BuESO-1.0, the broken pristine vitrimer films were used directly for subsequent reprocessing without further pulverizing. These fragments were sandwiched between two

Teflon® sheets and pressed at 230 °C and 5 MPa for 1 h. The mechanical properties of the resulting reprocessed films were determined. The same process was repeated five times, and the mechanical properties of the reprocessed films were recorded as a function of reprocessing time.

2.4.7 Observation of self-healing behaviors and shape memory properties. The self-healing behaviors of OHESO-1.0 and BuESO-1.0 were investigated using a BX53F2 optical microscope (Olympus, Japan). A piece of vitrimer film was first scratched using a razor blade at room temperature. The initial average width of the crack was measured. It was then cured in an oven at predetermined temperatures higher than its T_g without external force. The width changes of the crack were observed as a function of healing time. The obtained optical microscope images were processed using ImageJ software.[56]

The shape memory behavior of OHESO-1.0 was investigated in a series of heating-and-reheating processes. A strip of OHESO-1.0 film was reshaped and recovered at $T = 100$ °C (above its T_g). Memory erasing and rewriting of the original specimen were also conducted at $T = 180$ °C. The details are discussed in the ESI.†

3 Results and discussion

3.1 Monomers and materials preparation

The diacid monomers DVA and BuDVA were synthesized *via* the hydrolysis of their dimethyl esters (*i.e.*, Me-DVA and Me-BuDVA, respectively). As shown in Fig. 2(a) and (b), the proton signals at $\delta \approx 3.9$ ppm, attributed to the methyl esters of Me-DVA or Me-BuDVA, have vanished compared with in the ^{1}H NMR spectra of Me-DVA and Me-BuDVA in our previous work.[12] Furthermore, the proton signals at δ >12 ppm ($\delta = 12.54$ and 12.88 ppm for DVA and BuDVA, respectively) were assigned to COOH protons. All other signals can be assigned to the corresponding protons, the details of which are provided in Section S1.

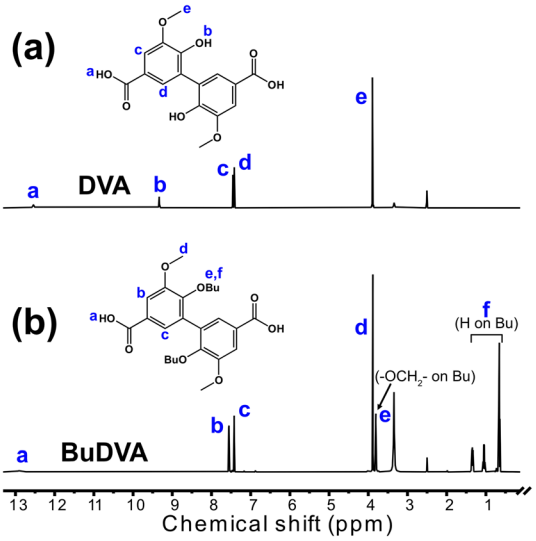

Fig. 2 ^{1}H NMR spectra of (a) DVA and (b) BuDVA in DMSO-d_6. The peaks are described in detail in the ESI.†

OHESO-x and BuESO-x vitrimers with $x = 0.7$, 1.0, and 1.5 were prepared in the present study. As shown in Fig. 1, all the BuESO-x films were transparent and homogeneous in color, OHESO-0.7 and OHESO-1.0 were semi-transparent, and OHESO-1.5 was opaque. It was considered that the BuDVA–ESO mixtures were prepared homogeneously, as mentioned in Section 2.3. In contrast, in the DVA–ESO mixtures, the free phenolic hydroxyl groups of the DVA molecules can form hydrogen bonds with the surrounding phenolic OH and/or carbonyl groups, and readily aggregate together. Consequently, the OHESO-x vitrimers were fabricated from immiscible DVA–ESO mixtures and were heterogeneous in appearance. These cured vitrimer films only swelled (or partially dissolved) in conventional organic solvents, so we studied their structures by swelling experiments and FT-IR spectroscopy. The swell ratios and gel contents of the vitrimers are listed in Table S1.† All the cured vitrimers exhibited high gel content values (>80%), which suggests that crosslinked networks had formed. For both OHESO-x and BuESO-x, vitrimers with $x = 1.0$ exhibited relatively high gel content values, which corresponded to their higher crosslink densities compared with those with $x = 0.7$ and 1.5. We attributed this result to the fact that the diacids did not completely react with the epoxy or hydroxyl groups (especially for vitrimers with $x = 1.5$), and therefore some free COOH groups remained. The unreacted COOH groups were also confirmed by FT-IR. During the swelling process, some linear segments, including unreacted monomers and uncrosslinked oligomers, were extracted from the vitrimer matrix. However, the quantitative relationship between the extracts and the difference in crosslinking density remains unclear.

The IR spectra of the monomers and cured OHESO-1.0 and BuESO-1.0 vitrimers are shown in Fig. 3, and the spectra of other vitrimers with $x = 0.7$ and 1.5 are shown in Fig. S2 and S3.† In the present study, we focused on three regions of the IR spectra: (1) 3800–3200 cm^{-1}, (2) 1780–1620 cm^{-1}, and (3) 870–800 cm^{-1}, which correspond to the absorption of hydroxyl groups, carbonyl groups, and epoxy groups, respectively.[55,57,58] In the 3800–3200 cm^{-1} region, there was broad absorption attributable to the free aliphatic OH groups, which derived from the ring-opening of the epoxy groups, of all the BuESO-x and OHESO-0.7 vitrimers (Fig. S2 and S3†). For the OHESO-1.5 and OHESO-1.0 vitrimers, these broad peaks overlapped with the absorption of the free phenolic OH and COOH groups. As mentioned before, because DVA molecules tend to aggregate together owing to the interaction of hydrogen bonds, some COOH groups remained unreacted during the curing process. In the 1780–1620 cm^{-1} region, there were peaks close to 1710 cm^{-1}, which were assigned to the carbonyl groups of the aromatic esters, between the peaks attributable to the carbonyl groups of ESO (1740 cm^{-1}) and those of the original aromatic acid (1685 and 1674 cm^{-1} for DVA and BuDVA, respectively). This indicates that the aromatic acid groups reacted with the epoxy groups (or reacted with the OH groups generated from ring-opening), and formed new ester bonds during curing and transesterification. Moreover, for all the OHESO-x and BuESO-1.5 vitrimers, there were shoulder peaks corresponding to the

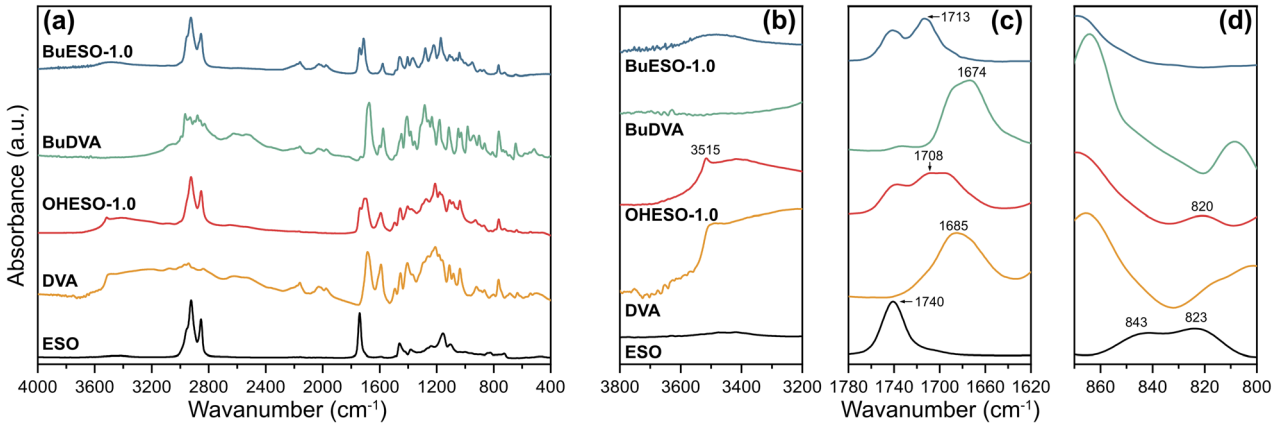

Fig. 3 (a) FT-IR spectra of ESO, DVA, OHESO-1.0, BuDVA, and BuESO-1.0, and enlarged views of regions (b) 3800–3200 cm^{-1}, (c) 1780–1620 cm^{-1}, and (d) 870–800 cm^{-1}.

COOH groups, which also suggests that some free COOH groups remained. In the 870–800 cm^{-1} region, the characteristic peaks attributable to epoxy groups (843 and 823 cm^{-1}) of the ESO vanished after curing in both the OHESO-*x* and BuESO-*x* vitrimers. This demonstrates that all the oxirane rings had been opened. The peak near 820 cm^{-1} produced by OHESO-*x*—the intensity of which increased as *x* increased—may have derived from the unreacted COOH groups. According to the previous research,[59,60] the homopolymerization of epoxy tends to occur at a relatively high level in a high epoxy/COOH environment (*i.e.*, off-stoichiometry) and at high curing temperatures, and the absorption of the C–O–C ether bond would appear in the regions of 1200–1100 cm^{-1}. In the present work, even in the cases of $x = 0.7$, we did not observe any distinguishable absorption of ether bonds. Overall, the results discussed above indicate that we had successfully prepared DVA/BuDVA–ESO vitrimers crosslinked by ester bonds. However, unreacted carboxylic acid groups remained in the matrices of the OHESO-*x* and BuESO-1.5 vitrimers.

3.2 Thermal properties of the vitrimers

The thermal properties of the vitrimer films were assessed by TGA and DMA. Table 2 lists the T_g, the temperature at which the mass loss became 5% ($T_{d5\%}$), and the temperature at which the maximum degradation rate occurred (T_{dmax}) of each film. The TGA and derivative TG (DTG) curves of the vitrimers are shown in Fig. 4. The thermal degradation of each vitrimer began at approximately 240 °C, which is similar to the degradation temperature of an epoxy resin.[61–63] The OHESO-*x* vitrimers had lower $T_{d5\%}$ values than the BuESO-*x* vitrimers because they had more free phenolic OH groups and unreacted COOH groups. The OHESO-*x* and BuESO-*x* vitrimers had comparable T_{dmax} values, but had lower $T_{d5\%}$ values than the aromatic bio-based polyesters, such as DVA-derived polyesters reported by us previously,[12,13] and furandicarboxylic acid-derived polyesters[5,64] (*e.g.*, $T_{d5\%}$ > 360 °C and T_{dmax} > 400 °C). These results may be explained as follows. At low temperatures, dehydration occurs much faster in OH-rich environments (*i.e.*, when a large number of aliphatic OH groups are generated by ring-opening). This causes faster chain scission in vitrimers.[63] At higher temperatures, vitrimers exhibit similar thermal degradation behaviors, such as β-hydrogen scission, to those of polyesters. Therefore, their T_{dmax} values occurred in the same temperature ranges.

The T_g values of the vitrimers were determined by DMA according to the peak temperatures of tan δ (the loss or damping factor) in the present study (Fig. 5). The T_g values of the OHESO-*x* and BuESO-*x* vitrimers were in the ranges 43–62 °C and 20–44 °C, respectively. The T_g values of OHESO-1.0 and

Table 2 Thermal and mechanical properties of the DVA/BuDVA–ESO vitrimers

Codes	T_g[a] (°C)	$T_{d5\%}$[b] (°C)	T_{dmax}[c] (°C)	σ_{max}[d] (MPa)	ε_{max}[e] (MPa)	E[f] (MPa)
OHESO-1.5	62	324	393	Not measured[g]		
OHESO-1.0	45	314	405	13.6 ± 1.1	13.6 ± 2	286 ± 49
OHESO-0.7	43	332	413	12.9 ± 1.4	23.6 ± 13.7	276 ± 81
BuESO-1.5	44	358	414	Not measured[g]		
BuESO-1.0	36	362	416	4.8 ± 0.6	69 ± 12	57 ± 11
BuESO-0.7	20	357	409	1.9 ± 0.3	116 ± 16	2.9 ± 0.5

[a] By DMA (peak temperature of tan δ). [b] The temperature at which the mass loss became 5%. [c] The temperature at which the maximum degradation rate occurred. [d] The maximum tensile strength. [e] The elongation at break. [f] The Young's modulus. [g] The films were too brittle to conduct tensile tests.

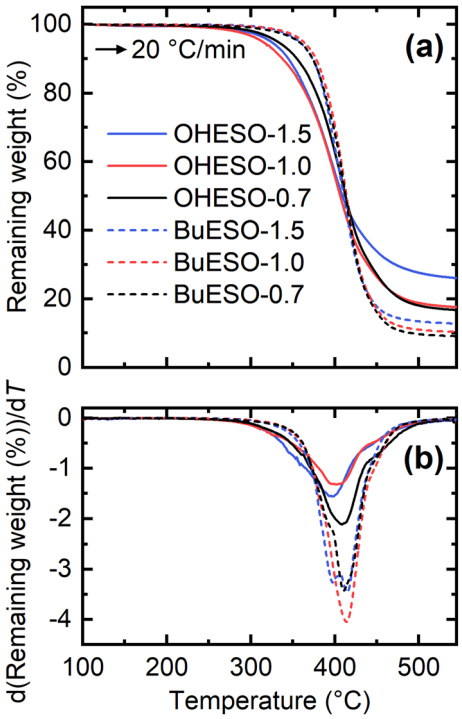

Fig. 4 (a) TGA and (b) derivative TG (DTG) thermograms produced by OHESO-*x* and BuESO-*x* at a heating rate of 20 °C min^{-1}.

OHESO-0.7 were almost equal, and were lower than that of OHESO-1.5. The T_g of BuESO-*x* increased as *x* increased. Generally, a high gel content corresponds to a high crosslinking density and T_g value of the crosslinked polymer. It was noticed that the order of T_gs was different from that of gel contents. The heterogeneity in vitrimer networks possibly caused this discrepancy. The T_gs of the OHESO-*x* vitrimers were higher than those of the BuESO-*x* vitrimers of the same *x* values, even though the gel contents of the BuESO-*x* vitrimers were higher than those of the OHESO-*x* vitrimers. This may be explained by the large free volume generated by the long Bu side chains of BuDVA, which endowed the molecular chains of the BuESO-*x* vitrimers with greater mobility. Furthermore, the hydrogen bonds formed by the free phenolic OH groups acted as physical crosslinks. As mentioned earlier, bio-based carboxylic acids and epoxy compounds have been used to develop vitrimer materials before. For example, Altuna *et al.*[28] prepared citric acid-ESO-based vitrimers (T_g < 30 °C), and Zhang *et al.*[44] prepared ozonated-lignin-based vitrimers (T_g > 90 °C). Therefore, high-rigidity monomers (*e.g.*, cyclic or aromatic monomers) with multiple functional groups (*i.e.*, more crosslinking points) can be used to prepare vitrimers with high T_g values.

3.3 Stress relaxation behavior

Stress relaxation is a common phenomenon of polymer materials. When a polymer is subjected to stress, its molecular chains tend to move to relax the stress, and relaxation becomes more rapid as the temperature increases.[65] In vitrimers, stress relaxation behavior is closely related to the bond-exchange reaction.[26] Therefore, we performed stress relaxation tests in the present work to confirm transesterification and evaluate the reaction rate. The stress relaxation curves of OHESO-1.0 and BuESO-1.0 at 170–200 °C, and those of the OHESO-*x* and BuESO-*x* vitrimers at 200 °C, are shown in Fig. 6.

We measured the G_t/G_0 change in the time range 0–20 000 s, where G_t and G_0 represent the relaxation moduli at times *t* and 0, respectively. Except for in the case of BuESO-1.0 at $T = 170$ and 180 °C, there was an apparent decrease in G_t/G_0 in each stress relaxation curve. This indicates that transesterification did occur during heating. Moreover, as shown in Fig. 6(a) and (b), the G_t/G_0 values decreased more rapidly as the temperature increased, corresponding to the increase in the transesterification rates. At $T = 200$ °C, BuESO-0.7 exhibited the most rapid decrease in G_t/G_0 [Fig. 6(d)]. This may have been because the concentration of free aliphatic OH groups was higher in BuESO-0.7 than in BuESO-1.0 and BuESO-1.5. Therefore, BuESO-0.7 underwent more rapid transesterification.[28]

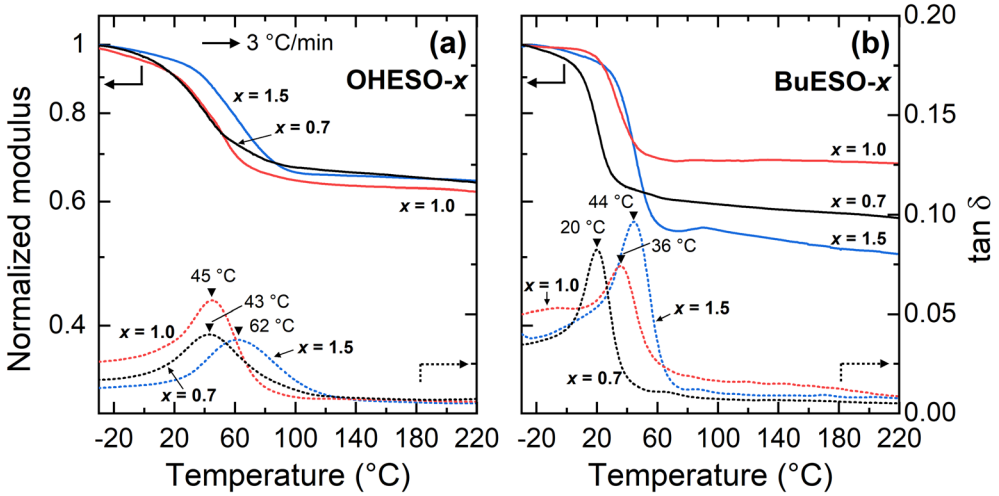

Fig. 5 DMA thermograms of (a) OHESO-*x* and (b) BuESO-*x* obtained at a heating rate of 3 °C min^{-1}. The T_g values are indicated by black triangles.

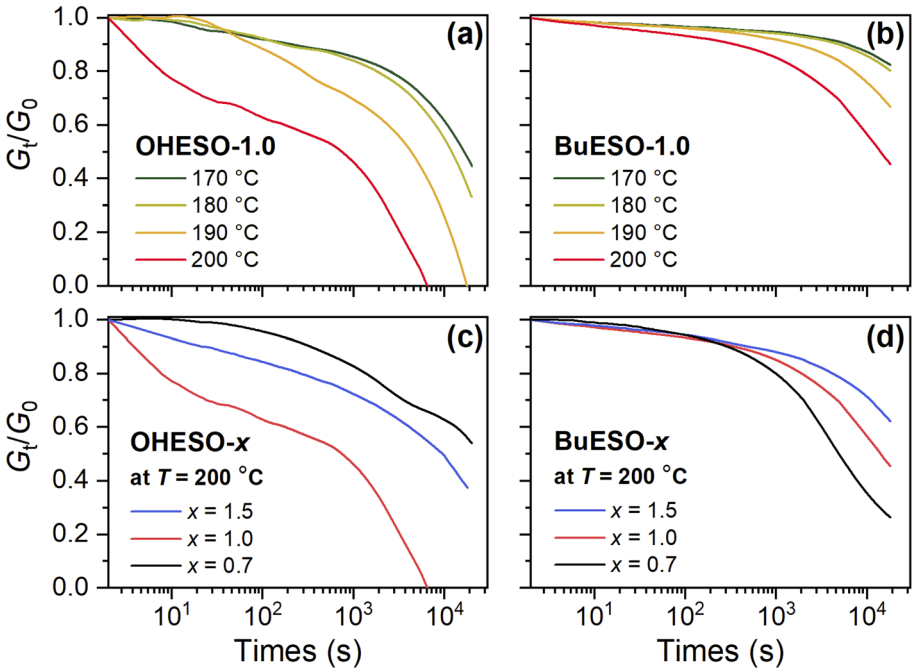

Fig. 6 Normalized stress relaxation curves of (a) OHESO-1.0 and (b) BuESO-1.0 at $T = 170–200$ °C, and normalized stress relaxation curves of (c) OHESO-x and (d) BuESO-x at $T = 200$ °C.

However, OHESO-0.7 and OHESO-1.0 had the lowest and highest relaxation rates of the OHESO-x vitrimers, respectively [Fig. 6(c)]. Unfortunately, we did not succeed in finding a plausible explanation for this irregular result, which may have been caused by the high heterogeneity of the OHESO-x matrix.

In a general Maxwell model, G_t/G_0 can be expressed by the simple exponential function:

$$G_t/G_0 = e^{\left(-\frac{t}{\tau}\right)}$$

where τ is the relaxation time, which is defined as the time when $G_t/G_0 = 1/e(0.37)$. However, in the present study, OHESO-x and BuESO-x exhibited more complex stress relaxation behaviors. According to several previous works,[66–68] we applied a stretched exponential function to fit the relaxation curves:

$$G_t/G_0 = e^{\left(-\frac{t}{\tau_{\text{fit}}}\right)^{\beta}} + c$$

Although this function cannot accurately describe the relaxation behaviors of the OHESO-x vitrimers in the time ranges $t < 10^2$ s, the relaxation of the vitrimers in the present work was relatively slow (*i.e.*, the G_t/G_0 values decreased to less than 0.5 at $t < 10^2$ s). Therefore, this function can be used to describe the relaxation behaviors in the long time ranges to evaluate the fitted relaxation time (τ_{fit}). The experimental data fitted well using this function, with R^2 values higher than 0.99. The best-fit values of τ_{fit}, and the β and c parameters are summarized in Table S2.†

The relaxation times of the vitrimers in the present study were obviously longer than those of other transesterification-based vitrimers, the τ values of which are typically in the range 10^2 to 10^3 s at T values close to 200 °C.[29,41,44,69] In other words, the transesterification rates of the DVA vitrimers were lower than those reported in most previous studies. To the best of our knowledge, only Altuna *et al.* have reported comparable slow relaxation behavior ($\tau > 20\,000$ s at $T = 160$ °C) in citric acid-ESO-based vitrimers.[28] There are many factors that affect the rates of stress relaxation, such as the types and concentrations of catalysts,[70] crosslinking densities,[71,72] branch numbers on crosslinker,[73] and polarity of the networks,[74] *etc.* We attributed the low relaxation rates of our vitrimers to the bulky and rigid chemical structures of the crosslinkers (*i.e.*, DVA and BuDVA), which reduced the movability of molecular chains and thus slowed down the reorganization of networks.

We calculated the approximate activation energy (E_a) of the transesterification reaction using the Arrhenius equation:[26,70]

$$\ln(\tau_{\text{fit}}) = -\ln A + \frac{E_a}{RT}$$

where R is the gas constant. The E_a values of OHESO-1.0 and BuESO-1.0 were 111.8 ± 18.7 and 118.6 ± 22.7 kJ mol^{-1}, respectively, which were higher than the value (≈90 kJ mol^{-1}) reported by Leibler *et al.*[70] This suggests that the OHESO-x and BuESO-x vitrimers underwent slow transesterification during heating as a consequence of the high activation barrier.

3.4 Mechanical properties of the pristine and reprocessed vitrimer films

The stress–strain curves of OHESO-x and BuESO-x ($x = 0.7$ and 1.0) are shown in Fig. 7, and their mechanical properties are summarized in Table 2. BuESO-1.0 had higher $\sigma_{\max}$ and E values, but lower $\varepsilon_{\max}$ values than BuESO-0.7, which agreed with

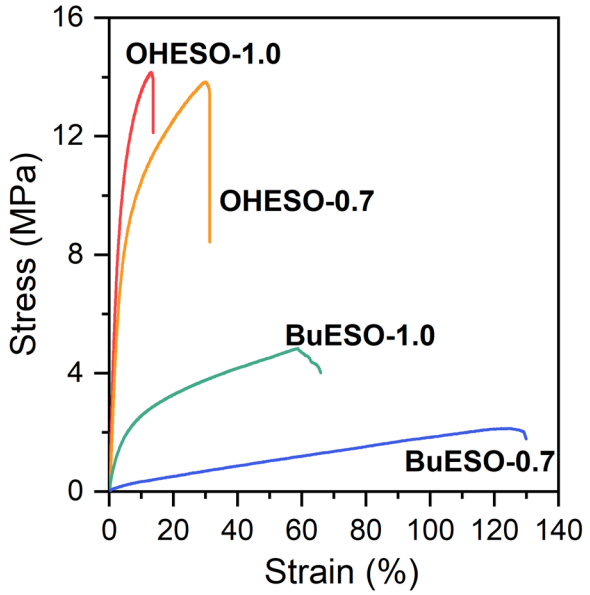

Fig. 7 Stress–strain curves of OHESO-*x* and BuESO-*x* vitrimer films (*x* = 0.7 and 1.0).

the result that BuESO-1.0 had a higher crosslink density. However, OHESO-1.0 had σ_{max} and E values that were only slightly higher than those of OHESO-0.7. This resembled their respective T_g relationships (the T_g of OHESO-1.0 was only slightly higher than that of OHESO-0.7). The increase in x had a more pronounced effect on the thermal and mechanical properties of BuESO-x compared with OHESO-x. Although the crosslink density of OHESO-1.0 was higher than that of OHESO-0.7, the unreacted and aggregated DVA moieties acted as defects, and caused a deterioration in the material properties. Therefore, OHESO-1.5 and BuESO-1.5 (noted that there were also unreacted COOH groups remained in BuESO-1.5) became too brittle for tensile tests.

One of the attractive properties of vitrimers is that they can be reprocessed and remolded at the high-temperatures at which bond exchange occurs. Therefore, vitrimers can be used to develop recyclable thermosets. In the present study, we investigated the mechanical properties of reprocessed OHESO-1.0 and BuESO-1.0 vitrimer films over five reprocessing cycles using the method described in Section 2.4. Images and stress–strain curves of the reprocessed films, and the retention of their mechanical properties after reprocessing, are shown in Fig. 8. The σ_{max}, ε_{max}, and E values are summarized in Table S3.† After reprocessing, the films were still coherent and self-standing, but became softer (especially the OHESO-1.0 film), and darkened in color compared with the pristine films. Similar cases have been reported previously.[41,49] The σ_{max} and E values of OHESO-1.0 and BuESO-1.0 decreased to 40–50% of their original values during reprocessing. The ε_{max} of the reprocessed BuESO-1.0 fluctuated between 70% and 110% of its original value, whereas that of the reprocessed OHESO-1.0 increased by more than 140% of its original value after three cycles of processing. This may be attributed to the decrease in crosslink density owing to thermal degradation at the high reprocessing temperature (230 °C), which was confirmed by reduced intensities of hydroxyl group absorption *via* FT-IR (Fig. S7 and S8†). This deterioration of mechanical properties can be improved by grinding the fragments into fine powders or prolonging the curing time, although it should be noted that thermal degradation should also be taken into account.[75] Using chemical methods to recycle vitrimer materials is also a good way of avoiding thermal degradation.[41,49,76] These results suggest that although the reprocessed DVA-derived vitrimers cannot be used

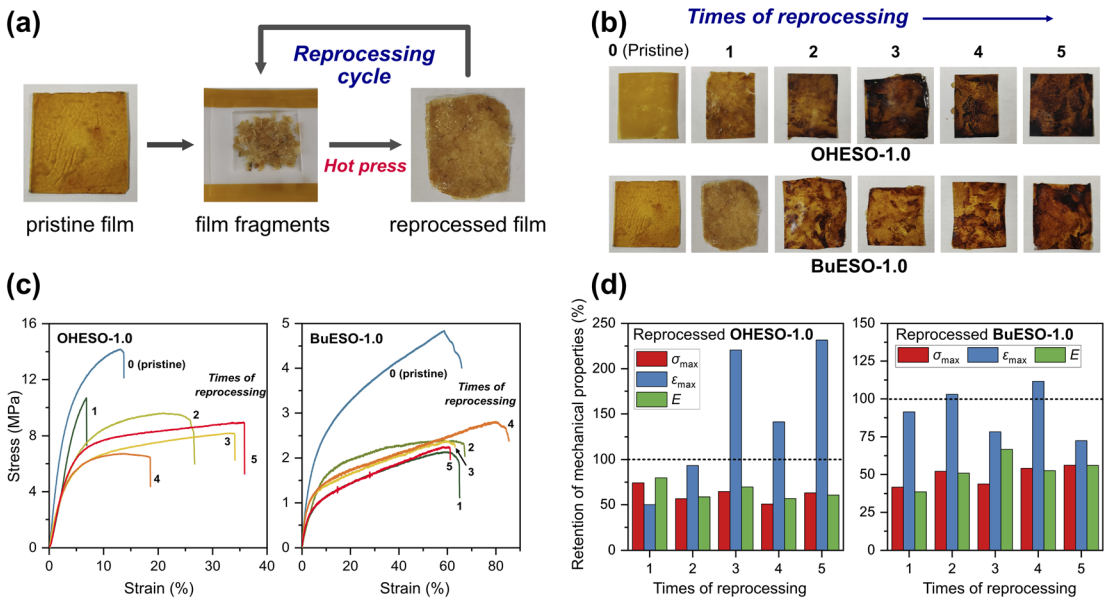

Fig. 8 (a) Reprocessing the vitrimer films. (b) Images of the OHESO-1.0 and BuESO-1.0 films obtained whilst reprocessing them five times. (c) Stress–strain curves of the pristine and reprocessed OHESO-1.0 and BuESO-1.0 films. (d) Retention rates of the mechanical properties of the reprocessed vitrimer films. The retention rates at 100% are indicated by dashed lines.

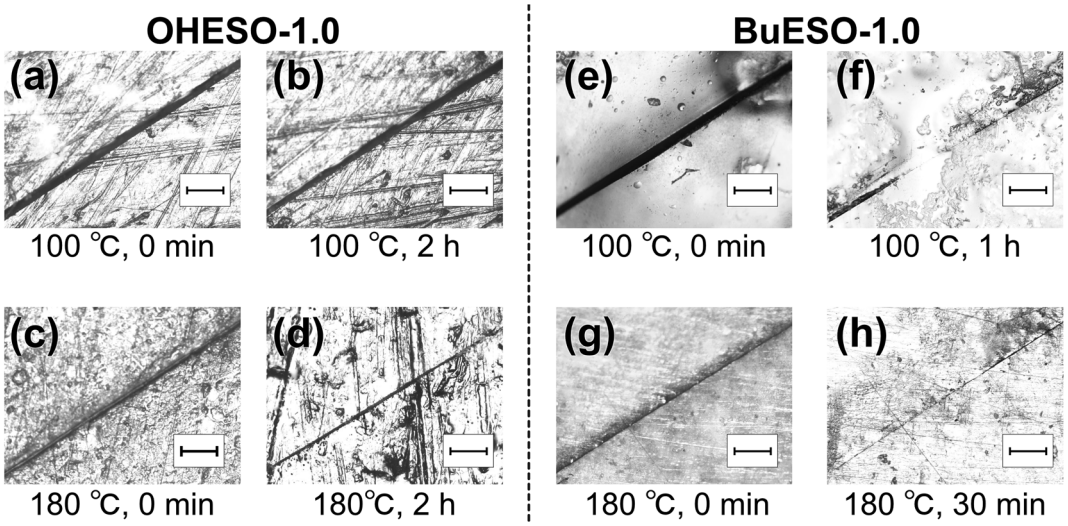

Fig. 9 Optical microscope images of (a–d) OHESO-1.0 and (e–h) BuESO-1.0 films healed at $T = 100$ and 180 °C. The scale bar represents 200 μm.

for the same application as the pristine vitrimers, owing to their inferior properties, they had better reprocessability and recyclability compared to traditional thermosets.

3.5 Self-healing property

Self-healing is a characteristic of dynamically crosslinked polymers. Bond exchange occurs during heating, which induces the rearrangement of molecular chains near the cracks. Consequently, the molecular chains refill the cracks, and the matrix material is healed. As shown in Fig. 9, we investigated the self-healing behaviors of OHESO-1.0 and BuESO-1.0 at $T =$ 100 and 180 °C in the present work.

At $T = 100$ °C [Fig. 9(a), (b), (e), and (f)], the crack in OHESO-1.0 was barely repaired after 2 h. In contrast, the crack width in BuESO-1.0 decreased from approximately 53 μm to approximately 7 μm in 1 h. Over 85% of the crack was healed (on the basis of crack width). OHESO-1.0 only exhibited self-healing at high temperatures. At $T = 180$ °C, [Fig. 9(c), (d), (g), and (h)] the crack width of OHESO-1.0 decreased slowly from approximately 20 to 15 μm over 2 h, whereas the crack in BuESO-1.0 was almost completely healed after 30 min. Obviously, BuESO-1.0 exhibited much higher repair rates at a wide range of temperatures compared with OHESO-1.0. This can be attributed to the hydrogen bonds formed by the free phenolic OH groups in OHESO-1.0. As mentioned previously, hydrogen bonds act as physical crosslinks, and hinder the movement of molecular chains, thereby slowing self-healing. In contrast to previous reports,[77,78] we did not observe complete healing in either OHESO-1.0 or BuESO-1.0, confirming the slow transesterification rates of our vitrimers (*i.e.*, their E_a values were relatively high).

Conclusions

In the present study, we prepared two series of bio-based vitrimers, *i.e.*, OHESO-*x* and BuESO-*x*, by curing DVA or BuDVA with ESO in the presence of a zinc-containing catalyst. Each vitrimer exhibited satisfactory thermal stability ($T_{d5\%}$ > 300 °C). Depending on their side chains and *x* values, the T_g values, Young's moduli, maximum elongation values, and tensile strengths of the vitrimers were in the ranges 20–62 °C, 3–286 MPa, 13–116%, and 2–14 MPa, respectively. As a result of the hydrogen bonds formed by the free phenolic hydroxyl groups and unreacted carboxylic acid groups remaining in the OHESO-*x* vitrimers, and the large free volumes generated by the butyl side chains in the BuESO-*x* vitrimers, the OHESO-*x* vitrimers had higher T_g, Young's modulus, and maximum tensile strength values than the BuESO-*x* vitrimers with the same *x* values. At temperatures approaching 200 °C, both series of vitrimers exhibited stress relaxation resulting from dynamic bond exchange reactions (*i.e.*, transesterification). We also investigated the shape memory, self-healing, and reprocessability behaviors of OHESO-1.0 and BuESO-1.0. After reprocessing (up to five cycles), the mechanical properties of the reprocessed films recovered to approximately 50% of those of the pristine films.

This present work demonstrates the feasibility of using symmetrical bio-based aromatic divanillic acid to prepare dynamically crosslinked vitrimers with favorable material properties and reprocessability. It also provides some new insights into the use of biomass-derived feedstocks to develop sustainable adhesives, coatings, and alternatives to other conventional thermosetting materials. Further research on the preparation of homogenous vitrimer films, and improvements to their thermal and mechanical properties are required before they will be suitable for practical applications.

Author contributions

Yunfan Zhang: Conceptualization, Investigation, Writing – original draft, Funding acquisition. Yukiko Enomoto: Conceptualization, Supervision, Writing – review & editing, Funding acquisition. Tadahisa Iwata: Writing – review & editing, Supervision, Funding acquisition.

Conflicts of interest

There are no conflicts to declare.

Acknowledgements

We acknowledge the financial support of the JSPS KAKENHI [grant number JP 20K06159, to Y. E.] and the JST SPRING from the University of Tokyo [grant number JPMJSP2108, to Y. Z.]. We thank New Japan Chemical Co., Ltd for providing the epoxidized soybean oil, and Professor Tsuguyuki Saito and Associate Professor Tetsuo Yamaguchi (both from the University of Tokyo) for the use of the rheometer.

References

1 R. Mülhaupt, *Macromol. Chem. Phys.*, 2013, **214**, 159–174.
2 S. Ramesh Kumar, P. Shaiju, K. E. O'Connor and R. B. Padamati, *Curr. Opin. Green Sustainable Chem.*, 2020, **21**, 75–81.
3 E. Castro-Aguirre, F. Iniguez-Franco, H. Samsudin, X. Fang and R. Auras, *Adv. Drug Delivery Rev.*, 2016, **107**, 333–366.
4 S. A. Rafiqah, A. Khalina, A. S. Harmaen, I. A. Tawakkal, K. Zaman, M. Asim, M. N. Nurrazi and C. H. Lee, *Polymers*, 2021, **13**, 1436.
5 G. Z. Papageorgiou, D. G. Papageorgiou, Z. Terzopoulou and D. N. Bikiaris, *Eur. Polym. J.*, 2016, **83**, 202–229.
6 Z. Terzopoulou, L. Papadopoulos, A. Zamboulis, D. G. Papageorgiou, G. Z. Papageorgiou and D. N. Bikiaris, *Polymers*, 2020, **12**, 1209.
7 S. Zhang, Z. Cheng, S. Zeng, G. Li, J. Xiong, L. Ding and M. Gauthier, *J. Appl. Polym. Sci.*, 2020, **137**, 49189.
8 E. Xanthopoulou, Z. Terzopoulou, A. Zamboulis, L. Papadopoulos, K. Tsongas, D. Tzetzis, G. Z. Papageorgiou and D. N. Bikiaris, *ACS Sustainable Chem. Eng.*, 2021, **9**, 1383–1397.
9 T. Goto, T. Iwata and H. Abe, *Biomacromolecules*, 2019, **20**, 318–325.
10 Y. Enomoto and T. Iwata, *Polymer*, 2020, **193**, 122330.
11 K. Fujieda, Y. Enomoto, Y. Zhang and T. Iwata, *Polymer*, 2022, **257**, 125241.
12 Y. Zhang, Y. Enomoto and T. Iwata, *Polymer*, 2020, **203**, 122751.
13 Y. Zhang, Y. Enomoto and T. Iwata, *Polym. Degrad. Stab.*, 2021, **192**, 109706.
14 K. Yagura, Y. Enomoto and T. Iwata, *Polymer*, 2022, **256**, 125222.
15 K. Yagura, Y. Zhang, Y. Enomoto and T. Iwata, *Polymer*, 2021, **228**, 123907.
16 Y. Enomoto and T. Iwata, *Eur. Polym. J.*, 2021, **154**, 110526.
17 R. T. Nishimura, C. H. Giammanco and D. A. Vosburg, *J. Chem. Educ.*, 2010, **87**, 526–527.
18 A. Llevot, E. Grau, S. Carlotti, S. Grelier and H. Cramail, *J. Mol. Catal. B: Enzym.*, 2016, **125**, 34–41.
19 S. S. Kuhire, A. B. Ichake, E. Grau, H. Cramail and P. P. Wadgaonkar, *Eur. Polym. J.*, 2018, **109**, 257–264.
20 A. Llevot, E. Grau, S. Carlotti, S. Grelier and H. Cramail, *Polym. Chem.*, 2015, **6**, 7693–7700.
21 A. Llevot, E. Grau, S. Carlotti, S. Grelier and H. Cramail, *Polym. Chem.*, 2015, **6**, 6058–6066.
22 E. Savonnet, C. Le Coz, E. Grau, S. Grelier, B. Defoort and H. Cramail, *Front. Chem.*, 2019, **7**, 606.
23 E. Savonnet, E. Grau, S. Grelier, B. Defoort and H. Cramail, *ACS Sustainable Chem. Eng.*, 2018, **6**, 11008–11017.
24 J. Liu, L. Zhang, W. Shun, J. Dai, Y. Peng and X. Liu, *J. Polym. Sci.*, 2021, **59**, 1474–1490.
25 Q. Zhang, M. Song, Y. Xu, W. Wang, Z. Wang and L. Zhang, *Prog. Polym. Sci.*, 2021, **120**, 101430.
26 D. Montarnal, M. Capelot, F. Tournilhac and L. Leibler, *Science*, 2011, **334**, 965.
27 W. Denissen, J. M. Winne and F. E. Du Prez, *Chem. Sci.*, 2016, **7**, 30–38.
28 F. I. Altuna, V. Pettarin and R. J. J. Williams, *Green Chem.*, 2013, **15**, 3360–3366.
29 T. Liu, C. Hao, L. Wang, Y. Li, W. Liu, J. Xin and J. Zhang, *Macromolecules*, 2017, **50**, 8588–8597.
30 T. Liu, C. Hao, S. Zhang, X. Yang, L. Wang, J. Han, Y. Li, J. Xin and J. Zhang, *Macromolecules*, 2018, **51**, 5577–5585.
31 M. Capelot, D. Montarnal, F. Tournilhac and L. Leibler, *J. Am. Chem. Soc.*, 2012, **134**, 7664–7667.
32 J. J. Lessard, L. F. Garcia, C. P. Easterling, M. B. Sims, K. C. Bentz, S. Arencibia, D. A. Savin and B. S. Sumerlin, *Macromolecules*, 2019, **52**, 2105–2111.
33 W. Denissen, G. Rivero, R. Nicolaÿ, L. Leibler, J. M. Winne and F. E. Du Prez, *Adv. Funct. Mater.*, 2015, **25**, 2451–2457.
34 P. R. Christensen, A. M. Scheuermann, K. E. Loeffler and B. A. Helms, *Nat. Chem.*, 2019, **11**, 442–448.
35 A. Zych, J. Tellers, L. Bertolacci, L. Ceseracciu, L. Marini, G. Mancini and A. Athanassiou, *ACS Appl. Polym. Mater.*, 2021, **3**, 1135–1144.
36 M. Röttger, T. Domenech, R. van der Weegen, A. Breuillac, R. Nicolaÿ and L. Leibler, *Science*, 2017, **356**, 62–65.
37 Y. Nishimura, J. Chung, H. Muradyan and Z. Guan, *J. Am. Chem. Soc.*, 2017, **139**, 14881–14884.
38 C. A. Tretbar, J. A. Neal and Z. Guan, *J. Am. Chem. Soc.*, 2019, **141**, 16595–16599.
39 B. Krishnakumar, A. Pucci, P. P. Wadgaonkar, I. Kumar, W. H. Binder and S. Rana, *Chem. Eng. J.*, 2022, **433**, 133261.
40 D. J. Fortman, J. P. Brutman, G. X. De Hoe, R. L. Snyder, W. R. Dichtel and M. A. Hillmyer, *ACS Sustainable Chem. Eng.*, 2018, **6**, 11145–11159.
41 X. Yang, L. Guo, X. Xu, S. Shang and H. Liu, *Mater. Des.*, 2020, **186**, 108248.
42 Y. Zeng, J. Li, S. Liu and B. Yang, *Polymers*, 2021, **13**, 3386.
43 X. Feng, J. Fan, A. Li and G. Li, *ACS Sustainable Chem. Eng.*, 2020, **8**, 874–883.
44 S. Zhang, T. Liu, C. Hao, L. Wang, J. Han, H. Liu and J. Zhang, *Green Chem.*, 2018, **20**, 2995–3000.
45 C. Hao, T. Liu, S. Zhang, L. Brown, R. Li, J. Xin, T. Zhong, L. Jiang and J. Zhang, *ChemSusChem*, 2019, **12**, 1049–1058.
46 M. Qi, Y.-J. Xu, W.-H. Rao, X. Luo, L. Chen and Y.-Z. Wang, *RSC Adv.*, 2018, **8**, 26948–26958.

47 Q. Yu, X. Peng, Y. Wang, H. Geng, A. Xu, X. Zhang, W. Xu and D. Ye, *Eur. Polym. J.*, 2019, **117**, 55–63.
48 Y.-Y. Liu, J. He, Y.-D. Li, X.-L. Zhao and J.-B. Zeng, *Compos. Commun.*, 2020, **22**, 100445.
49 H. Memon, H. Y. Liu, M. A. Rashid, L. Chen, Q. R. Jiang, L. Y. Zhang, Y. Wei, W. S. Liu and Y. P. Qiu, *Macromolecules*, 2020, **53**, 621–630.
50 X.-L. Zhao, Y.-Y. Liu, Y. Weng, Y.-D. Li and J.-B. Zeng, *ACS Sustainable Chem. Eng.*, 2020, **8**, 15020–15029.
51 K. P. Cortés-Guzmán, A. R. Parikh, M. L. Sparacin, A. K. Remy, L. Adegoke, C. Chitrakar, M. Ecker, W. E. Voit and R. A. Smaldone, *ACS Sustainable Chem. Eng.*, 2022, **10**, 13091–13099.
52 S. Engelen, A. A. Wróblewska, K. De Bruycker, R. Aksakal, V. Ladmiral, S. Caillol and F. E. Du Prez, *Polym. Chem.*, 2022, **13**, 2665–2673.
53 S. Grauzeliene, M. Kastanauskas, V. Talacka and J. Ostrauskaite, *ACS Appl. Polym. Mater.*, 2022, **4**, 6103–6110.
54 A. Roig, P. Hidalgo, X. Ramis, S. De la Flor and À. Serra, *ACS Appl. Polym. Mater.*, 2022, **4**, 9341–9350.
55 J. F. Scholtes and O. Trapp, *Angew. Chem., Int. Ed.*, 2019, **58**, 6306–6310.
56 C. A. Schneider, W. S. Rasband and K. W. Eliceiri, *Nat. Methods*, 2012, **9**, 671–675.
57 A. Adhvaryu and S. Z. Erhan, *Ind. Crops Prod.*, 2002, **15**, 247–254.
58 J. S. Lupoi, S. Singh, R. Parthasarathi, B. A. Simmons and R. J. Henry, *Renew. Sustain. Energy Rev.*, 2015, **49**, 871–906.
59 S. Chappuis, P. Edera, M. Cloitre and F. Tournilhac, *Macromolecules*, 2022, **55**, 6982–6991.
60 Q.-A. Poutrel, J. J. Blaker, C. Soutis, F. Tournilhac and M. Gresil, *Polym. Chem.*, 2020, **11**, 5327–5338.
61 L.-H. Lee, *J. Polym. Sci., Part A: Gen. Pap.*, 1965, **3**, 859–882.
62 M. Natarajan and S. C. Murugavel, *Polym. Bull.*, 2017, **74**, 3319–3340.
63 P.-Y. Kuo, L. de Assis Barros, Y.-C. Sheen, M. Sain, J. S. Y. Tjong and N. Yan, *J. Anal. Appl. Pyrolysis*, 2016, **117**, 199–213.
64 Z. Terzopoulou, V. Tsanaktsis, M. Nerantzaki, D. S. Achilias, T. Vaimakis, G. Z. Papageorgiou and D. N. Bikiaris, *J. Anal. Appl. Pyrolysis*, 2016, **117**, 162–175.
65 A. V. Tobolsky, *J. Appl. Phys.*, 1956, **27**, 673–685.
66 E. E. L. Maassen, J. P. A. Heuts and R. P. Sijbesma, *Polym. Chem.*, 2021, **12**, 3640–3649.
67 Z. Song, Z. Wang and S. Cai, *Mech. Mater.*, 2021, **153**, 103687.
68 K. S. Fancey, *J. Mater. Sci.*, 2005, **40**, 4827–4831.
69 J. P. Brutman, P. A. Delgado and M. A. Hillmyer, *ACS Macro Lett.*, 2014, **3**, 607–610.
70 M. Capelot, M. M. Unterlass, F. Tournilhac and L. Leibler, *ACS Macro Lett.*, 2012, **1**, 789–792.
71 M. Chen, H. Si, H. Zhang, L. Zhou, Y. Wu, L. Song, M. Kang and X.-L. Zhao, *Macromolecules*, 2021, **54**, 10110–10117.
72 M. Hayashi and R. Yano, *Macromolecules*, 2020, **53**, 182–189.
73 T. Isogai and M. Hayashi, *Macromolecules*, 2022, **55**, 6661–6670.
74 S. K. Schoustra, T. Groeneveld and M. M. J. Smulders, *Polym. Chem.*, 2021, **12**, 1635–1642.
75 K. Yu, P. Taynton, W. Zhang, M. L. Dunn and H. J. Qi, *RSC Adv.*, 2014, **4**, 10108–10117.
76 W. Zhao, Z. Feng, Z. Liang, Y. Lv, F. Xiang, C. Xiong, C. Duan, L. Dai and Y. Ni, *ACS Appl. Mater. Interfaces*, 2019, **11**, 36090–36099.
77 M. Hayashi, R. Yano and A. Takasu, *Polym. Chem.*, 2019, **10**, 2047–2056.
78 W.-Q. Yuan, G.-L. Liu, C. Huang, Y.-D. Li and J.-B. Zeng, *Macromolecules*, 2020, **53**(22), 9847–9858.